INTECH
open science | open minds

OPEN ACCESS
ARTICLE

International Journal of Advanced Robotic Systems

Dynamic Coupling Analysis of a Spatial 6-DOF Electro-Hydraulic Parallel Manipulator Using a Modal Decoupling Method

Regular Paper

Chifu Yang[1,*] and Junwei Han[1]

1 Dept. of Mechanical and Electrical Engineering, Harbin Institute of Technology, Harbin, Heilongjiang, China
* Corresponding author E-mail: cfyang1008@gmail.com

Received 10 May 2012; Accepted 12 Nov 2012

DOI: 10.5772/55028

Abstract The workspace of a spatial 6-DOF electro-hydraulic parallel manipulator is strongly coupled, due to its multi-closed-loop kinematic structure and the coupling complicates motion planning and control of the parallel manipulator. This paper clearly analyses the strong dynamic coupling property in the workspace of a spatial 6-DOF parallel manipulator, using modal decoupling theory and a frequency responses characteristics analysis method. The dynamic model of a spatial 6-DOF electro-hydraulic parallel manipulator is expressed with the Kane method and hydromechanics principles. The modal analysis method is used to establish the map between strong coupling workspace and decoupled modal space and the dynamic coupling relationship and coupling strength between workspaces are exactly revealed. The quantitative evaluation index of dynamic coupling is presented. Moreover, the relationship between dynamic coupling effects and input is discussed through applying frequency characteristics analysis. Experimental results show the workspace of the parallel manipulator is strongly coupled and the coupling property is coincident with theoretical results.

Keywords Parallel Manipulator, Dynamic Coupling, Modal Analysis, Frequency Response Characteristics

1. Introduction

Parallel manipulators have been extensively investigated due to their high force-to-weight, high stiffness, high accuracy and widespread applications in various fields, such as high fidelity simulators, space docking motion systems and machine tools [1-4]. A spatial 6-DOF electro-hydraulic parallel manipulator is often used as a spatial multi-DOF motion and load system with a heavy payload for its special loading capacity. Although a spatial electro-hydraulic parallel manipulator has many excellent characteristics, it has a key disadvantage that strong dynamic coupling, resulting from the dynamics of the parallel manipulator, has always existed in the workspace

of a manipulator. The dynamic coupling can result in the interactive effects of performance between all six degrees-of-freedom; in other words, the performance of each channel can affect and restrict the performance of other channels. The dynamic coupling effects of a spatial 6-DOF electro-hydraulic parallel manipulator can be summarized in two aspects. One is that the 6-DOF electric-hydraulic parallel manipulator is a six-input-six-output system, but each channel is coupled with another due to dynamic coupling, hence, it is very hard to realize the independent controller design in each channel of workspace or joint space. The other is the coupling error related to the dynamic coupling effect. With respect to the spatial 6-DOF electro-hydraulic parallel manipulator, the entire control performance and potential is limited and restricted by dynamic coupling. To develop a decoupled structure or decoupled control technique for a electro-hydraulic parallel manipulator, the analysis of dynamic coupling is very important and significant.

Despite of the high potential of performances offered by a parallel manipulator, it is yet to achieve the desired success because of its high kinematic and dynamic coupling [5]. In current design theories, decoupling the functional requirements of a mechanical system has become a basic design principle [6]. This design principle is also applicable in robotics and it can provide significant advantages in design, modelling, trajectory planning and control [7]. In the last thirty years, impressive progress has been made in studies on coupling in 6-DOF parallel manipulators. Many researchers have proposed different decoupling methods for parallel manipulators and parallel kinematic structures. Hoffman [8] proposed a unitary decoupling matrix to analyse a hydraulic driven flight simulator motion system, a Stewart platform, in combination with decentralized feedback. He showed that the unitary matrix can be used in a state transformation matrix, which decouples the 12th order system into a 2nd system, each having the same structure as the 1-DOF hydraulically driven mechanical systems. Feng et al. [9] employed cross coupling error technology to develop synchronized tracking control for parallel manipulators. Innocenti et al. [10] proposed a 6-DOF parallel manipulator with decoupled motion, in which three links share a common ball joint so that the position of the end-effector is only controlled by these three links. Lallemand et al. [11] introduced a 6-DOF decoupled 2-Delta PR with the external Delta robot responsible for the translation of the end-effector and the internal Delta robot for controlling the orientation of the end-effector through one limb that allows only free translation but no rotation. Shim et al. [12] reported a decoupled 3-PRPS 6-DOF parallel manipulator with the two prismatic joints of each limb representing the actuators. McInroy et al. [13] and Li et al. [14] developed a control strategy for fault tolerant precision hexapod pointing using a method that employed single-input-single-output (SISO) plants by the combination of hexapod geometry, mechanical design and sensor positioning with proper sensor to actuator decoupling transformation. McInroy [15] developed two decoupling algorithms by combining static input-output transformations with a hexapod geometric design. Chen et al. [16] presented a decoupling algorithm with fewer constraints on the geometric and payload design using a joint space mass-inertia matrix based on the constrained least squares and the symmetric positive definite estimation method. Zabalza et al. [17] proposed a 6-DOF parallel manipulator, which decouples the 3-DOF planar motion and the other 3- DOF spatial motion by using three modified Scott's mechanisms. Yang et al. [18] proposed a 6-DOF 3-RPRS decoupled parallel manipulator, in which the three planar motions and the other three motions are independently controlled. Jin et al. [19] studied the effects of constraint errors on parallel manipulators with decoupled motion and proposed a method to identify the constraint errors and evaluate the effects of the errors on decoupling characteristics of the parallel manipulator.

With the above-mentioned decoupling methods, the lengths of the actuators of the decoupled parallel manipulator seem to be controlled independently. However, the system is, in fact, highly interactive. Therefore, the resultants dynamics of the parallel manipulator can still be highly nonlinear and highly coupled. The force of one actuator will generally induce reaction forces in all DOFs. Furthermore, the desired motion of the system requires the coordinated motion of all actuators.

The main aim of this paper is to provide theoretical foundation in order to develop a method to solve the dynamic coupling effects for a spatial 6-DOF parallel manipulator, via clearly revealing the dynamic coupling phenomenon, dynamic coupling relationship and the dynamic coupling strength of a spatial 6-DOF electro-hydraulic parallel manipulator with a novel coupling analysis approach. The mathematical model of the parallel manipulator is expressed under the Kane method and the hydrodynamics principle. The spatial 6-DOF parallel manipulator is treated as a vibration system and the free vibration equation is established. With the vibration equation, the modal analysis method is utilized to clearly analyse the dynamic coupling characteristics of a spatial 6-DOF parallel manipulator and the dynamic coupling evaluation matrix is used to reflect the coupling relationship and the coupling strength is defined. The experiment is carried out to analyse the dynamic coupling under the frequency responses characteristics method. In Section 2, the dynamic model of a spatial 6-DOF parallel manipulator is built. In Section 3, the dynamic coupling is analysed in theory. In Section 4, the

experiment results are given and discussed and the conclusion is drawn in Section 5.

2. Dynamic model of parallel manipulator

The spatial 6-DOF electro-hydraulic parallel manipulator is shown in Figure 1. Figure 2 explains the configuration. l_i (i=1,…,6) is the actuator length, a_i (i=1,…,6) is the upper gimbal coordinates in the body coordinate system and b_i (i=1,…,6) is the lower gimbal coordinates in the base coordinate system. The linear motions denote as surge (q_1), sway (q_2) and heave (q_3) along the X-Y-Z axis for the base coordinate system. The angular motions labelled as roll (q_4), pitch (q_5) and yaw (q_6) are Euler angles of the platform.

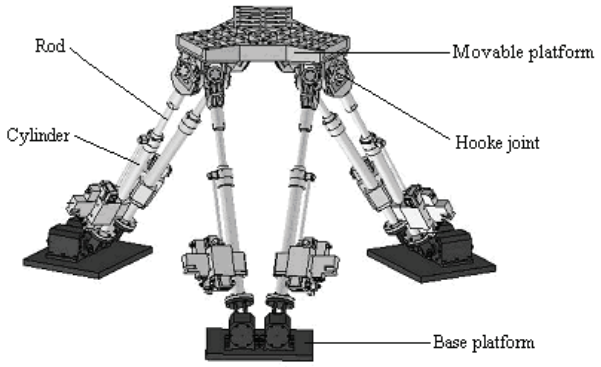

Figure 1. Spatial 6-DOF parallel manipulator

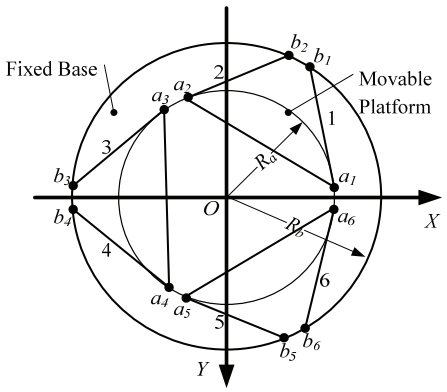

Figure 2. Definition of configuration parameter of parallel manipulator

The dynamics of the spatial 6-DOF parallel manipulator have been investigated [20-21] and in this section the dynamic model of the spatial 6-DOF parallel manipulator is derived by using the Kane method.

The body frame is fixed to the movable platform and its origin is the centre of mass of the movable platform. The inertial frame is fixed to the earth and its origin is the same as that of the body frame in the initial pose of the parallel manipulator. The linear motions labelled as surge (q_1), sway (q_2) and heave (q_3) are along the X-Y-Z axis in the inertial frame and the angular motions denoted as roll (q_4), pitch (q_5) and yaw (q_6) are Euler angles of the platform around the X-Y-Z axis, which is used to parameterize the rotation matrix $\boldsymbol{R}$:

$$\mathbf{R}=\begin{bmatrix} \mathrm{cq}_5\cdot\mathrm{cq}_6 & \mathrm{cq}_6\cdot\mathrm{sq}_5\cdot\mathrm{sq}_4-\mathrm{sq}_6\cdot\mathrm{cq}_4 & \mathrm{sq}_6\cdot\mathrm{sq}_4+\mathrm{cq}_6\cdot\mathrm{sq}_5\cdot\mathrm{cq}_4 \\ \mathrm{sq}_6\cdot\mathrm{cq}_5 & \mathrm{cq}_6\cdot\mathrm{cq}_4+\mathrm{sq}_6\cdot\mathrm{sq}_5\cdot\mathrm{sq}_4 & \mathrm{sq}_6\cdot\mathrm{sq}_5\cdot\mathrm{cq}_4-\mathrm{cq}_6\cdot\mathrm{sq}_4 \\ -\mathrm{sq}_5 & \mathrm{cq}_5\cdot\mathrm{sq}_4 & \mathrm{cq}_5\cdot\mathrm{cq}_4 \end{bmatrix} \quad (1)$$

where cq,sq represents $\cos\mathrm{q},\sin\mathrm{q}$, respectively. The upper joint coordinate $\boldsymbol{a}_i$ in the body frame can be transformed into that in the inertial frame via $\boldsymbol{R}$ and is given as:

$$\mathbf{a}_\mathrm{i}^{\,\mathrm{L}}=\mathbf{R}\mathbf{a}_\mathrm{i}+\mathbf{c} \quad i=1,2,\ldots,6 \quad (2)$$

where $\mathbf{c}$ is the coordinate of the origin of the body frame in the inertial frame. The linear velocity of the upper joint in the inertial frame is calculated by:

$$\mathbf{v}_{\mathrm{ai}}^{\,\mathrm{L}}=\dot{\mathbf{R}}\mathrm{a}_\mathrm{i}+\dot{\mathbf{c}}=\boldsymbol{\omega}^{\mathrm{L}}\times\mathbf{R}\mathrm{a}_\mathrm{i}+\dot{\mathbf{c}}=\begin{bmatrix}\mathbf{I} & \mathbf{R}\tilde{\mathrm{a}}_\mathrm{i}\mathbf{R}^{\mathrm{T}}\end{bmatrix}\dot{\bar{\mathbf{q}}}=\mathbf{J}_{\mathrm{ai},\bar{\mathrm{q}}}\dot{\bar{\mathbf{q}}} \quad (3)$$

where $\boldsymbol{\omega}^{\mathrm{L}}$ is the angular velocity of the movable platform in the inertial frame. The angular velocity of leg $\boldsymbol{\omega}_{\mathrm{li}}$ around the lower joint is expressed as:

$$\boldsymbol{\omega}_{\mathrm{li}}=\mathbf{l}_{\mathrm{ni}}\times\mathbf{v}_{\mathrm{ai}}/|\,|\mathbf{l}_\mathrm{i}|\,|_2=\mathbf{J}_{\mathrm{wi,ai}}\mathbf{v}_{\mathrm{ai}} \quad (4)$$

where $\mathbf{l}_{\mathrm{ni}}$ is the unit leg vector and $\mathbf{l}_\mathrm{i}$ is the leg length vector in the inertial frame, formulated by:

$$\mathbf{l}_\mathrm{i}=\mathbf{a}_\mathrm{i}^{\,\mathrm{L}}-\mathbf{b}_\mathrm{i}=\mathbf{R}\mathbf{a}_\mathrm{i}+\mathbf{c}-\mathbf{b}_\mathrm{i} \quad i=1,2,\ldots,6 \quad (5)$$

where $\boldsymbol{b}_i$ is the coordinate of the lower joint in the inertial frame. By the derivative of (5) along the leg direction, the linear velocity of the leg is described as:

$$\dot{\mathbf{l}}_\mathrm{i}=\mathbf{l}_{\mathrm{ni}}\cdot\mathbf{v}_{\mathrm{ai}}=\mathbf{l}_{\mathrm{ni}}^{\,\mathrm{T}}(\boldsymbol{\omega}^{\mathrm{L}}\times\mathbf{R}\mathbf{a}_\mathrm{i}+\dot{\mathbf{c}}) \quad (6)$$

The unit leg vector $\mathbf{l}_{\mathrm{ni}}$ in the inertial frame is expressed as:

$$\mathbf{l}_{\mathrm{ni}}=\mathbf{l}_{\mathrm{ni}}/|\,|\mathbf{l}_{\mathrm{ni}}|\,|_2=(\mathbf{R}\mathbf{a}_\mathrm{i}+\mathbf{c}-\mathbf{b}_\mathrm{i})/|\,|\mathbf{R}\mathbf{a}_\mathrm{i}+\mathbf{c}-\mathbf{b}_\mathrm{i}|\,|_2 \quad i=1,2,\ldots,6 \quad (7)$$

The matrix form of (6) for six legs can be given as:

$$\dot{\mathbf{L}}=\mathbf{J}_{\mathrm{l}\bar{\mathrm{q}}}\dot{\bar{\mathbf{q}}}=\begin{bmatrix}\mathbf{L}_\mathrm{n}^{\,\mathrm{T}} & (\mathbf{R}\mathbf{A}\times\mathbf{L}_\mathrm{n})^{\mathrm{T}}\end{bmatrix}\dot{\bar{\mathbf{q}}} \quad (8)$$

where $\mathbf{J}_{\mathrm{l}\bar{\mathrm{q}}}$ is a Jacobian matrix between the generalized velocity of the movable platform and the leg velocity, $\boldsymbol{A}$ is the upper joint coordinate matrix, $\mathbf{L}_\mathrm{n}$ is the unit leg direction matrix and $\dot{\bar{\mathbf{q}}}$ is the generalized velocity of the movable platform. The relationship of $\boldsymbol{\omega}^{\mathrm{L}}$ and the Euler angles is given by:

$$\boldsymbol{\omega}^{\mathrm{L}}=\begin{bmatrix}\omega_1^{\,\mathrm{L}}\\ \omega_2^{\,\mathrm{L}}\\ \omega_3^{\,\mathrm{L}}\end{bmatrix}=\mathbf{R}\cdot\boldsymbol{\omega}^{\mathrm{b}}\cdot\boldsymbol{\pi}(\beta)=\mathbf{R}\begin{bmatrix}1 & 0 & -\mathrm{sq}_5\\ 0 & \mathrm{cq}_4 & \mathrm{cq}_5\mathrm{sq}_4\\ 0 & -\mathrm{sq}_4 & \mathrm{cq}_5\mathrm{cq}_4\end{bmatrix}\begin{bmatrix}\dot{\mathrm{q}}_4\\ \dot{\mathrm{q}}_5\\ \dot{\mathrm{q}}_6\end{bmatrix} \quad (9)$$

where $\boldsymbol{\omega}^b$ is the angular velocity of the movable platform in the body frame.

The linear velocity $\mathbf{v}_{aci}$ of the centre of mass of the *i*th rod can be calculated with $\boldsymbol{\omega}_{li}$ and $\mathbf{v}_{ai}$ and described as:

$$\mathbf{v}_{aci} = \mathbf{v}_{ai} - \boldsymbol{\omega}_{li} \times (r_a \mathbf{l}_{ni}) = (\mathbf{I} - r_a \mathbf{P}_{\mathbf{l}_{ni}} / |\,|\mathbf{l}_i|\,|)\mathbf{v}_{ai} = \mathbf{J}_{aci,ai}\mathbf{v}_{ai} \quad (10)$$

where $\mathbf{P}_{\mathbf{l}_{ni}}$ is a projected operator, r_a is the distance between the centre of mass of the rod and the upper joint and $\mathbf{J}_{aci,ai}$ is the Jacobian matrix between the upper joint velocity and the velocity of the centre of mass of the rod.

The inertial force of the leg resulting from linear motions is described as:

$$\mathbf{J}_{ai,\bar{q}}{}^{T}\left(\mathbf{J}_{aci,ai}{}^{T} m_a \dot{\mathbf{v}}_{aci} + \mathbf{J}_{bci,ai}{}^{T} m_b \dot{\mathbf{v}}_{bci}\right) = \mathbf{F}_{lvi} \quad (11)$$

where m_a and m_b are the mass of the rod and cylinder of the leg, v_{bci} is the velocity of the centre of mass of the cylinder and $\mathbf{J}_{bci,ai}$ is a Jacobian matrix.

$$\mathbf{v}_{bci} = \mathbf{J}_{bci,ai}\mathbf{J}_{ai,\bar{q}}\dot{\bar{\mathbf{q}}} \quad (12)$$

In the inertial frame, the inertial force of the leg stemming from rotation is formulated as:

$$\mathbf{J}_{ai,\bar{q}}{}^{T}\mathbf{J}_{wi,ai}{}^{T}\left((\mathbf{I}_{ai} + \mathbf{I}_{bi})\dot{\boldsymbol{\omega}}_{li} + \boldsymbol{\omega}_{li} \times (\mathbf{I}_{ai} + \mathbf{I}_{bi})\boldsymbol{\omega}_{li}\right) = \mathbf{F}_{lai} \quad (13)$$

where $\mathbf{I}_{ai}, \mathbf{I}_{bi}$ are the inertia matrices of the rod and the cylinder in the inertial frame, respectively.

The inertial force and the moment of the movable platform can be given as:

$$m_p \ddot{\mathbf{c}} = \mathbf{F}_p \quad (14)$$

$$\mathbf{I}_p \dot{\boldsymbol{\omega}} + \boldsymbol{\omega} \times \mathbf{I}_p \boldsymbol{\omega} = \mathbf{M}_p \quad (15)$$

where m_p is the mass of the movable platform, $\boldsymbol{\omega}$ is the angular velocity of the movable platform in the inertial frame and $\mathbf{I}_p$ is the inertia matrix of the movable platform in the inertial frame.

The generalized active force of the parallel manipulator can be expressed as:

$$\mathbf{J}_{l\bar{q}}{}^{T}\mathbf{F}_a + \mathbf{G} = \mathbf{F}_{active} \quad (16)$$

where $\mathbf{F}_a$ is the leg output force and $\mathbf{G}$ is the gravity term, given by:

$$\mathbf{G}(\mathbf{q}) = \begin{bmatrix} m_p \mathbf{g}^T & 0_{1\times 3} \end{bmatrix}^T + \mathbf{J}_{ai,\bar{q}}{}^{T}(\mathbf{J}_{aci,ai}{}^{T} m_a + \mathbf{J}_{bci,ai}{}^{T} m_b)\mathbf{g} \quad (17)$$

By combining equations (1)-(17), the full dynamic equation of the spatial 6-DOF parallel manipulator is derived by using the Kane method:

$$\mathbf{M}(\mathbf{q})\ddot{\bar{\mathbf{q}}} + \mathbf{C}(\mathbf{q}, \dot{\bar{\mathbf{q}}})\dot{\bar{\mathbf{q}}} + \mathbf{G}(\mathbf{q}) = \mathbf{J}_{l\bar{q}}{}^{T}(\mathbf{q})\mathbf{F}_a \quad (18)$$

where $\boldsymbol{M}$ is the mass matrix and $\boldsymbol{C}$ is the centrifugal term:

$$\mathbf{M}(\mathbf{q}) = \begin{bmatrix} m_p \mathbf{I}_{3x3} & 0 \\ 0 & \mathbf{I}_p \end{bmatrix} + \sum_{i=1}^{6} \left\{ \mathbf{J}_{ai,\bar{q}}{}^{T} \begin{bmatrix} \mathbf{J}_{aci,ai}{}^{T} m_a \mathbf{J}_{aci,ai} + \\ \mathbf{J}_{bci,ai}{}^{T} m_b \mathbf{J}_{bci,ai} + \\ \mathbf{J}_{wi,ai}{}^{T}(\mathbf{I}_a + \mathbf{I}_b)\mathbf{J}_{wi,ai} \end{bmatrix} \mathbf{J}_{ai,\bar{q}} \right\} \quad (19)$$

$$\mathbf{C}(\mathbf{q}, \dot{\bar{\mathbf{q}}}) = \begin{bmatrix} 0_{3x3} & 0 \\ 0 & \tilde{\boldsymbol{\omega}}\mathbf{I}_p \end{bmatrix} + \sum_{i=1}^{6} \left\{ \begin{array}{l} \mathbf{J}_{ai,\bar{q}}{}^{T} \begin{bmatrix} \mathbf{J}_{aci,ai}{}^{T} m_a \, d(\mathbf{J}_{\mathbf{aci,ai}}\mathbf{J}_{ai,\bar{q}})/dt + \\ \mathbf{J}_{bci,ai}{}^{T} m_b \, d(\mathbf{J}_{\mathbf{bci,ai}}\mathbf{J}_{ai,\bar{q}})/dt \end{bmatrix} + \\ \mathbf{J}_{ai,\bar{q}}{}^{T}\mathbf{J}_{wi,ai}{}^{T} \begin{bmatrix} (\mathbf{I}_{ai} + \mathbf{I}_{bi})\, d(\mathbf{J}_{wi,ai}\mathbf{J}_{ai,\bar{q}})/dt + \\ \mathbf{J}_{\mathbf{wi,ai}}\mathbf{J}_{ai,\bar{q}}\dot{\bar{\mathbf{q}}} \times (\mathbf{I}_{ai} + \mathbf{I}_{bi})\mathbf{J}_{wi,ai}\mathbf{J}_{ai,\bar{q}} \end{bmatrix} \end{array} \right\} \quad (20)$$

An electro-hydraulic system is the power mechanism of the spatial 6-DOF parallel manipulator. It employs six servo-valves and unsymmetrical actuators. The dynamics of the hydraulic system are written as:

$$q_{Li} = c_d \cdot w \cdot x_{vi} \sqrt{\frac{1}{\rho}(p_s - \mathrm{sign}(x_{vi})p_{Li})} \quad (21)$$

$$q_{Li} = A_1 \cdot \dot{l}_i + c_{tc} p_{Li} + c_{tic} p_s + \frac{(1+n^4)\cdot A_1 \cdot L}{2(1+n^2)(1+n^3)E}\dot{p}_{Li} \quad (22)$$

$$A_1 p_{Li} = F_{ai} + F_{fi} \quad (23)$$

where q_{Li} is the load flow of the *i*th hydraulic actuator, *w* is the area gradient, x_{vi} is the valve position of the *i*th servovalve, ρ is the fluid density, p_s is the supply pressure, A_1 is the effective acting area of the piston, A_2 is the effective acting area of no rod chamber, c_{tc}, c_{tic} are the leakage coefficients, p_{Li} is the load pressure of the *i*th actuator, $p_{Li} = F_{Li} / A_1$, E is the bulk modulus of the fluid, c_d is the flow coefficient, *n* is the ratio of the area, $n = A_2 / A_1$, F_{ai} is the net actuator output force of the *i*th leg and F_{fi} is the friction in the *i*th actuator.

3. Dynamic coupling analysis

A spatial 6-DOF electro-hydraulic parallel manipulator can be treated as a spatial six dimensional vibration system with six hydraulic springs along the direction of an actuator. The centrifugal term, gravity term and friction can be neglected in free vibration differential equations of the parallel manipulator. Therefore, the dynamic equation (18) can be represented as:

$$\mathbf{M}(\mathbf{q})\ddot{\bar{\mathbf{q}}} = \mathbf{J}_{l\bar{q}}{}^{T}(\mathbf{q})\mathbf{F}_s \quad (24)$$

where $\mathbf{F}_s$ is the relative spring force corresponding to the inertial pose:

$$F_{si} = K_{li}\Delta l_i, \quad i = 1, \cdots, 6 \quad (25)$$

where K_{li} is the stiffness of the *i*th hydraulic spring and Δl_i is relative position of the *i*th hydraulic spring. Equation (25) can be rewritten in matrix form:

$$\mathbf{F}_s = \mathbf{K}_l \Delta \mathbf{l} \tag{26}$$

where

$\mathbf{F}_s = \begin{bmatrix} \mathbf{F}_{s1} & \cdots & \mathbf{F}_{s6} \end{bmatrix}^T$,

$\Delta \mathbf{l} = \begin{bmatrix} \Delta l_1 & \cdots & \Delta l_6 \end{bmatrix}^T$,

$\mathbf{K}_l = \mathrm{diag}\begin{bmatrix} K_{l1} & \cdots & K_{l6} \end{bmatrix}$.

$$\Delta \mathbf{l} = \mathbf{J}_{l\bar{q}} \Delta \bar{\mathbf{q}} \tag{27}$$

where

$$\Delta \bar{\mathbf{q}} = \begin{bmatrix} \Delta q_1 & \Delta q_2 & \Delta q_3 & \Delta \bar{q}_4 & \Delta \bar{q}_5 & \Delta \bar{q}_{61} \end{bmatrix}^T.$$

Then, equation (24) is written as:

$$\mathbf{M}(\mathbf{q})\ddot{\bar{\mathbf{q}}} + \mathbf{J}_{l\bar{q}}{}^T \mathbf{K}_l \mathbf{J}_{l\bar{q}} \Delta \bar{\mathbf{q}} = 0 \tag{28}$$

Defining:

$$\mathbf{K}_q = \mathbf{J}_{l\bar{q}}{}^T \mathbf{K}_l \mathbf{J}_{l\bar{q}} \tag{29}$$

We can obtain the differential equation of free vibration of the spatial 6-DOF electro-hydraulic parallel manipulator, which is expressed as:

$$\mathbf{M}(\mathbf{q})\ddot{\bar{\mathbf{q}}} + \mathbf{K}_q \bar{\mathbf{q}} = 0 \tag{30}$$

With (26), the vibration mode equation can be derived as:

$$\left(\mathbf{K}_q - \omega_n{}^2 \mathbf{M}\right)\mathbf{X} = 0 \tag{31}$$

where ω_n is the natural frequency and ***X*** is the vibration amplitude, which is also the eigenvector of (31). Equation (31) can be also rewritten as:

$$\left(\mathbf{S} - \lambda \mathbf{E}\right)\mathbf{X} = 0 \tag{32}$$

where $\mathbf{S}$ is a coefficient matrix, $\mathbf{S} = \mathbf{M}^{-1}\mathbf{K}_q$, $\lambda = \omega_n{}^2$. By using an eigenvalue decomposition algorithm, all eigenvectors can be obtained and the modal matrix can be derived.

$$\mathbf{\Phi} = \begin{bmatrix} \mathbf{X}_1 & \mathbf{X}_2 & \cdots & \mathbf{X}_6 \end{bmatrix} \tag{33}$$

Obviously, the real modal matrix has orthogonal characteristics. With mass matrix $\mathbf{M}$ and stiffness matrix $\mathbf{K}_q$, we can get:

$$\mathbf{\Phi}^T \mathbf{M} \mathbf{\Phi} = \hat{\mathbf{M}} \tag{34}$$

$$\mathbf{\Phi}^T \mathbf{K}_q \mathbf{\Phi} = \hat{\mathbf{K}}_q \tag{35}$$

where $\hat{\mathbf{M}}_l$ is a diagonal modal matrix and $\hat{\mathbf{K}}_q$ is a diagonal modal stiffness matrix. Hence, the vibration equation (30) can expressed as:

$$\mathbf{\Phi}\hat{\mathbf{M}}\mathbf{\Phi}^T \ddot{\bar{\mathbf{q}}} + \mathbf{\Phi}\hat{\mathbf{K}}_q \mathbf{\Phi}^T \bar{\mathbf{q}} = 0 \tag{36}$$

Defining:

$$\mathbf{\Phi}^T \bar{\mathbf{q}} = \hat{\mathbf{q}} \tag{37}$$

where $\hat{q}$ is the modal coordinate. Then, equation (36) can be rewritten as:

$$\hat{\mathbf{M}}\ddot{\hat{\mathbf{q}}} + \hat{\mathbf{K}}_q \hat{\mathbf{q}} = 0 \tag{38}$$

By using modal space transformation, the strong dynamic coupling system of the spatial 6-DOF parallel manipulator is decoupled into an uncoupled system described in its modal space and the dynamic coupling relationship of the workspace can be explicitly formulated with transposed modal matrix $\mathbf{\Phi}^T$.

The modal matrix can be described as:

$$\mathbf{\Phi}^T = \begin{bmatrix} \Phi_{11} & \cdots & \Phi_{16} \\ \vdots & \ddots & \vdots \\ \Phi_{61} & \cdots & \Phi_{66} \end{bmatrix} \tag{39}$$

If the number of the elements $\Phi_{ij} \neq 0$ in each row is more than two, the DOFs corresponding to the number of non-zero elements in each row are coupled. Further assuming that $\Phi_{1i}, \cdots, \Phi_{6i} (1 \le i \le 6) \neq 0$ is the maximal elements of each row.

Defining:

$$\chi = \begin{bmatrix} \chi_{11} & \cdots & \chi_{16} \\ \vdots & \ddots & \vdots \\ \chi_{61} & \cdots & \chi_{66} \end{bmatrix} = \begin{bmatrix} \Phi_{11}/\Phi_{1i} & \cdots & \Phi_{16}/\Phi_{6i} \\ \vdots & \ddots & \vdots \\ \Phi_{61}/\Phi_{1i} & \cdots & \Phi_{66}/\Phi_{6i} \end{bmatrix} \tag{40}$$

Therefore, the dynamic coupling evaluation matrix of coupling relationship and coupling strength among DOFs is established. If the number of the element $\chi_{ij} \neq 0$ in each row of χ is more than two, the DOFs corresponding to the number of non-zero elements in each row are coupled. Excepting for $\chi_{ij} = 1$, the stronger coupling appears in the DOF $\chi_{ij} = 1$ and the DOF $\left|\chi_{ij}\right|_{\max} \neq 1$.

4. Experiment and discussion

With a view to proving the proposed dynamic coupling analysis method and confirming the presented coupling evaluation index and further discussing the dynamic coupling characteristics of the spatial 6-DOF parallel manipulator, the experiment is carried out on a real

parallel manipulator. The experimental parallel manipulator is shown in Figure 3.

Figure 3. Experimental electro-hydraulic parallel manipulator

Through using the proposed dynamic coupling approach, the coupling evaluation matrix in its zero position of the experimental parallel manipulator can be derived.

$$\chi = \begin{bmatrix} 1 & 0 & 0 & 0 & -0.2711 & 0 \\ -0.0807 & 0 & 0 & 0 & 1 & 0 \\ 0 & 0 & 1 & 0 & 0 & 0 \\ 0 & 0.0772 & 0 & 1 & 0 & 0 \\ 0 & -1 & 0 & 0.2677 & 0 & 0 \\ 0 & 0 & 0 & 0 & 0 & 1 \end{bmatrix} \quad (41)$$

In terms of the coupling evaluation matrix (41) of the parallel manipulator, the directions of surge and pitch are coupled, as well as sway and roll directions in the zero-position of the 6-DOF parallel manipulator, but there is no coupling in heave and yaw directions.

In the zero-position of the spatial 6-DOF parallel manipulator, 6 random signals are applied to the experimental parallel manipulator. With the frequency responses characteristics analysis method, the coupling frequency response characteristics curves between one input and all six outputs of the experimental parallel manipulator are illustrated in Figure 4.

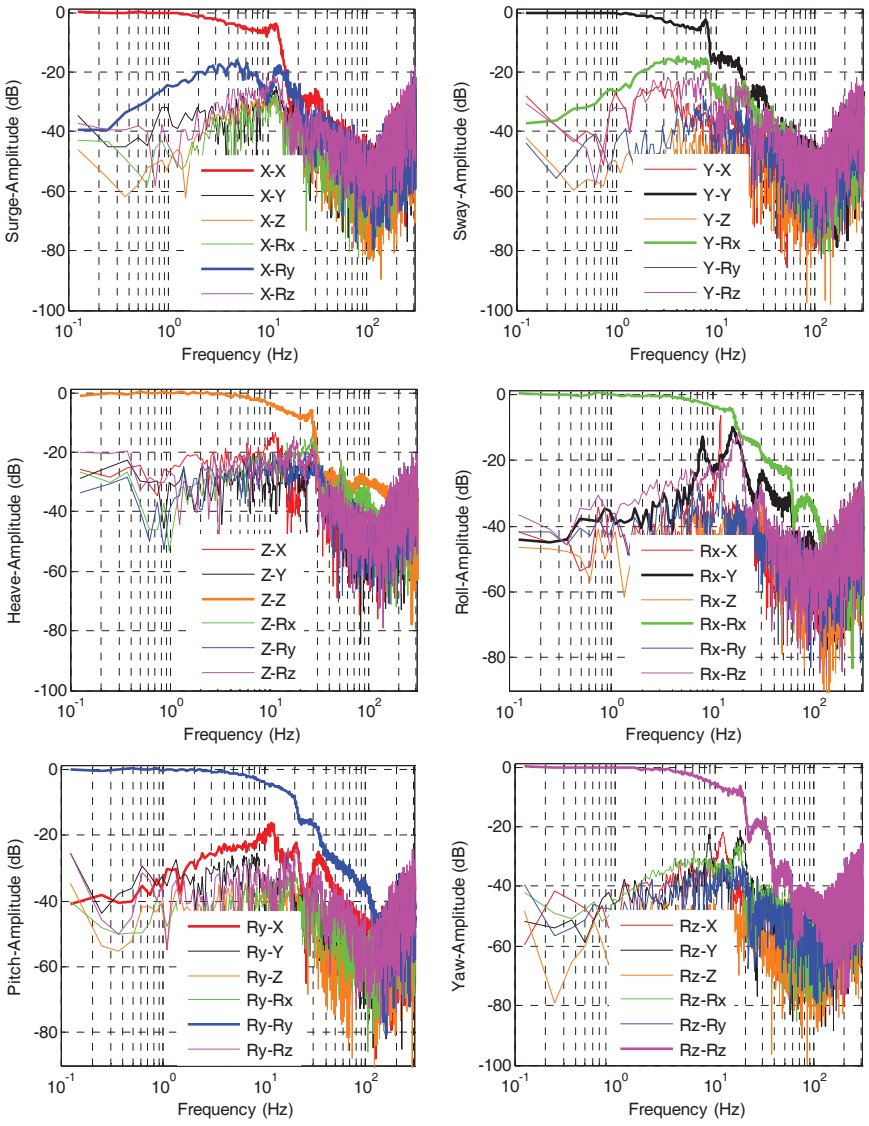

Figure 4. Experimental coupling characteristics in DOFs of the parallel manipulator

As can be seen from Figure 4, the coupling exists in the surge and pitch, sway and roll directions in the zero-position of the parallel manipulator. The maximal coupling also appears in surge and pitch, sway and roll directions, which are coincident with the theoretical results. Furthermore, the experimental results also show that the coupling effects are related to the amplitude and frequency of the inputs of the parallel manipulator. In the low frequency region, the coupling effects are small. With increasing frequency, the coupling effects become greater. When the frequency is close to the natural frequency, the coupling effects attain the maximum value. As the frequency of movement increase, the coupling effects decrease. For the same frequency, the influences of coupling increase with the raising of the amplitude of the inputs.

For the other pose, $q_3 = 0.2\text{m}$, the evaluation matrix is changed to:

$$\chi = \begin{bmatrix} 1 & 0 & 0 & 0 & -0.2656 & 0 \\ -0.0805 & 0 & 0 & 0 & -1 & 0 \\ 0 & 0 & 1 & 0 & 0 & 0 \\ 0 & 0.0769 & 0 & 1 & 0 & 0 \\ 0 & -1 & 0 & 0.2609 & 0 & 0 \\ 0 & 0 & 0 & 0 & 0 & 1 \end{bmatrix} \quad (42)$$

According to the coupling evaluation matrix (42) of the parallel manipulator, the coupling relationship is not changed, but the coupling strength is altered for the heave motion. The experiment results are demonstrated in Figure 5.

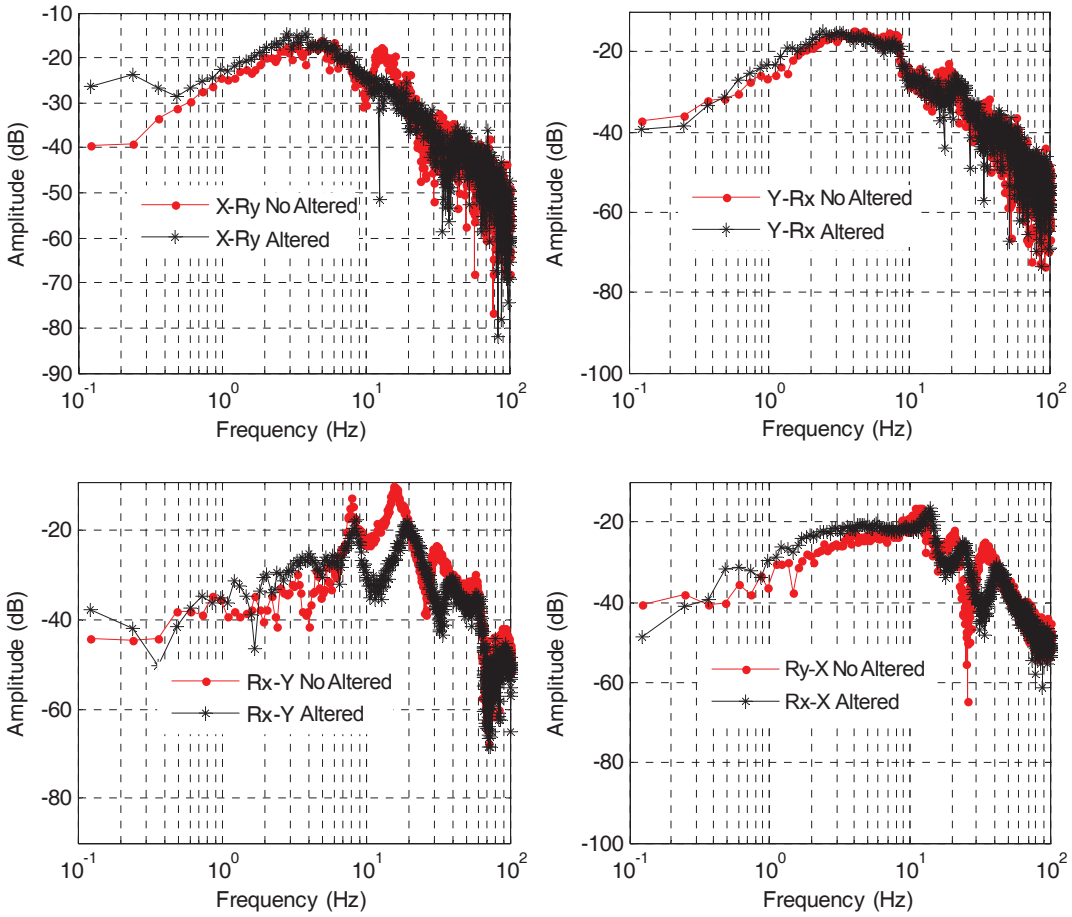

Figure 5. Experimental coupling characteristics in DOFs of the parallel manipulator

Comparisons illustrate that the experimental results are coincident with the theoretical results and the coupling relationship is not varied; only the coupling strength is changed.

5. Conclusions

This paper investigates the dynamic coupling of a spatial 6-DOF electro-hydraulic parallel manipulator, with a view to derive the theoretical foundation of developing an effective method to eliminate the effects of dynamic coupling on a spatial 6-DOF electro-hydraulic parallel manipulator. The evaluation matrix of the dynamic coupling relationship and dynamic coupling strength between six DOFs are gained via the modal decoupling technique. The dynamic coupling characteristics are clearly revealed in theory and experimentally with a modal analysis method and a frequency response characteristics analysis method. The surge direction is coupled with pitch direction, the sway is coupled with

roll and there is no coupling in both heave and yaw. Furthermore, the dynamic coupling effect is small in low frequency regions but can become greater with increasing frequency. When the frequency is close to the natural frequency, the coupling effects attain the maximum value. As the frequency of movement increases, the coupling effects decrease. Under the same frequency, the influences of dynamic coupling increase with the raising of the amplitude of inputs. Moreover, the defined evaluation index of dynamic coupling of a spatial 6-DOF parallel manipulator provides a guide to structure and control design to remove the dynamic coupling effects.

6. Acknowledgements

This research was supported by 921 Manned Space Project of China, and the National Natural Science Foundation of China (51205392, 51105094). The authors would like to thank CAST, NSFC and to thank the Editor, Associate Editors and anonymous reviewers for their constructive comments.

7. References

[1] Merlet J. P. (2006) Parallel robots. Netherlands: Kluwer Academic Publisher.

[2] Yang C. F., Huang Q. T., Jiang H. Z., Peter O. O., Han J. W. (2010) PD control with gravity compensation for hydraulic 6-DOF parallel manipulator. Mechanism and Machine Theory. 45: 666-677.

[3] Yang C. F., Huang Q. T., Han J. W. (2012) Decoupling control for spatial six-degree-of-freedom electro-hydraulic parallel robot. Robotics and Computer-Integrated Manufacturing. 28: 14-23.

[4] Jin Y., Chen I. M., Yang G. L. (2009) Kinematic design of a family of 6-DOF partially decoupled parallel manipulators. Mechanism and Machine Theory. 44: 912-922.

[5] Briot S., Arakelian V., Guegan S. (2009) PAMINSA: A new family of partially decoupled parallel manipulators. Mechanism and Machine Theory. 44: 425-444.

[6] Sun N. P. (1990) The Principles of Design. USA: Oxford University Press.

[7] Gogu G. (2007) Rangularity: Cross coupling kinetostatic index for parallel robots. 12th IFToMM World Congress, Besancon France, Jun 18-21.

[8] Hoffman R. (1979) Dynamics and control of a flight simulator motion system. Proceedings of the Canadian Conference of Automatic Control.

[9] Feng L., Koren Y., Borenstein. J (1993) Cross coupling motion controller for mobile robots. IEEE Control Systems Magazine. 13(6): 35-43.

[10] Innocenti C., Parenti-Castelli V. (1992) Direct kinematics of the 6-4 fully parallel manipulator with position and orientation uncoupled. Tzafestas S. G., editors. Robotic Systems: Advanced Techniques and Applications. London: Kluwer Academic Publisher. Part 1, pp. 3-10.

[11] Lallemand J. P., Goudali A., Zeghloul S. (2000) The 6-DOF 2-Delta parallel robot. Robotica. 15: 407-416.

[12] Shim J. H., Kwon D. S., Cho H. S. (1999) Kinematic analysis and design of a six D.O.F. 3-PRPS in-parallel manipulator. Robotica. 17: 269–281.

[13] McInroy J. E., Brien J. F., Neat G. W. (1999) Precise, fault tolerant pointing using Stewart platform. IEEE/ASME Transaction on Mechatronics. 4(1): 91-95.

[14] Li X, McInroy J. E., Hamann J. C. (2003) Optimal fault tolerant control of flexure jointed hexapods for applications requiring less than 6 DOF. Proceedings of the IEEE conference on Decision and Control, Sydney Australia. 4: 3337-3338.

[15] McInroy J. E. (2002) Modeling and design of flexure jointed Stewart platforms for control purposes. IEEE/ASME Transactions on Mechatronics. 7(1): 95-99.

[16] Chen Y. X., McInroy J. E. (2004) Decoupled control of flexure-jointed hexapods using estimated joint-space mass-inertia matrix. IEEE Transactions on Control Systems Technology. 12(3): 413-421.

[17] Zabalza J., Ros J., Gil J. J., Pintor J. M., Jimenez J. M. (2002) Tri-scott. A Micabo like 6 DOF quasi-decoupled parallel manipulator. Proceedings of the Workshop on Fundamental Issues and Future Research Directions for Parallel Mechanisms and Manipulators, Quebec City, Quebec, Canada.

[18] Yang G. I., Chen I. M., Chen W. H., Lin W. (2004) Kinematic design of a six-DOF parallel-kinematics machine with decoupled-motion architecture. IEEE Transactions on Robotics. 20(5): 876-887.

[19] Jin Y., Chen I. M. (2006) Effects of constraint errors on parallel manipulators with decoupled motion. Mechanism and Machine Theory. 14: 912-928.

[20] Yang C. F., He J. F., Han J. W., Liu X. C. (2009) Real-time state estimation for spatial six- degree-of-freedom linearly actuated parallel robots. Mechatronics. 19: 1026-1033.

[21] Yang C. F., Zheng S. T., Han J. W., Peter O. O. (2012) Dynamic modeling and computational efficiency analysis for a spatial 6-DOF parallel motion system. Nonlinear Dynamics. 67: 1007-1022.